

Effect of atomic order on the electrical resistivity of $\text{Co}_x\text{Fe}_{100-x}$ alloys

P. P. Freitas* and L. Berger

Physics Department, Carnegie-Mellon University, Pittsburgh, Pennsylvania 15213

(Received 5 August 1987)

We measured the electrical resistivity at 4.2 K of a series of $\text{Co}_x\text{Fe}_{100-x}$ alloys in the ordered and disordered state. For $30 < x < 40$ at. % Co the resistivity increases upon ordering as expected when an energy gap occurs at the Fermi level. For $40 < x < 70$ at. % Co the resistivity decreases upon ordering due to an increase of the electron relaxation time. For two samples with $x=38$ and $x=48$ at. % Co we measured $\rho(T_Q, T)$ at temperatures $T=4.2, 77,$ and 295 K after quenching the samples in salt water from several temperatures T_Q around the ordering temperature T_o . For the first sample, $\rho(T_Q, 4.2 \text{ K})$ increases for $T_Q < T_o$ and accordingly $d\rho(T_Q, 4.2 \text{ K})/dT_Q$ has a strong negative anomaly at T_o . At high temperatures and in equilibrium, $\rho(T)$ decreases upon ordering and $d\rho/dT$ has a positive anomaly at T_o . This crossover from a gap-dominated to a relaxation-time-dominated critical behavior is induced by increasing the measuring temperature T , therefore exciting electrons across the energy gap. From the dependence of $\rho(T_Q, T)$ on T we estimate the gap width to be around 45 meV. For $x=50$ at. % Co both $\rho(T_Q, 4.2 \text{ K})$ and $\rho(T)$ decrease upon ordering. Here the gapless behavior of the resistivity is due to the particular topology of the Fermi surface.

I. INTRODUCTION

The behavior of the zero-field resistivity of a binary alloy,

$$\rho = m^* / e^2 n_{\text{eff}} \tau, \quad (1)$$

near an order-disorder phase transition depends on the possible variation with atomic order of the electron relaxation time, τ , and of the effective number of carriers per unit volume, n_{eff} . Here, m^* is the electron effective mass. If n_{eff} does not change, and if inelastic collisions are neglected, the atomic-disorder resistivity can be written¹

$$\rho(T) / \rho_{\text{dis}} \propto \int d\Omega_q \int_0^{2K_F} \Gamma(\mathbf{q}, T) q^3 dq, \quad (2)$$

where

$$\Gamma(\mathbf{q}, T) = \sum_{\mathbf{R}} e^{i\mathbf{q}\cdot\mathbf{R}} \langle \sigma_0 \sigma_{\mathbf{R}} \rangle \quad (3)$$

and $d\Omega_q$ is an element of solid angle in q space. $\Gamma(\mathbf{q}, T)$ is the Fourier transform of the two-site correlation function, the direct analog of the spin-spin correlation function for an Ising antiferromagnet. Also, the σ_r are the site-occupation parameters as described by Cowley,² and ρ_{dis} is the atomic-disorder resistivity in the completely disordered state. Simons and Salamon³ followed an argument similar to that of Fisher and Langer⁴ (FL) to treat the correlation function for atomic disorder. They found that the anomaly in $d\rho/dT$ for an order-disorder system has the same form as that in the specific heat. In their theory, short-range concentration fluctuations at $q \sim 2K_F$ are dominant near the critical temperature. This leads to a smooth increase of the resistivity across the critical region and to a positive cusp in $d\rho/dT$ at the critical temperature T_o :

$$(1/\rho_{\text{dis}})(d\rho/dT)_{\text{FL}} \propto |\varepsilon|^{-\alpha}, \quad (4)$$

where $\varepsilon = (T - T_o)/T_o$ is the reduced temperature, and α is the critical exponent for the specific heat. Suezaki and Mori (SM)⁵ discussed the critical behavior of the resistivity of antiferromagnets and order-disorder systems, when long-range fluctuations are dominant. In their work, they used the Ornstein-Zernike approximation for the correlation function. Therefore their results are essentially those of a mean-field theory, and are not expected to be valid very close to T_o . They obtained for the relaxation time the following behavior:

$$1/\tau = A + B(1 - D|\varepsilon|^{2\beta}), \quad (5)$$

where β is the critical exponent for the long-range order parameter. This leads to an upward-pointing cusp in the resistivity at T_o , in opposition to the monotonic increase predicted by Fisher and Langer. The resistivity derivative becomes

$$(1/\rho_{\text{dis}})(d\rho/dT)_{\text{SM}} \sim |\varepsilon|^{2\beta-1}. \quad (6)$$

Notice that in a mean-field approximation Eq. (2) leads to

$$\rho(T) / \rho_{\text{dis}} = 1 - S^2(T). \quad (7)$$

Since the long-range order parameter S goes like $|\varepsilon|^\beta$ near and below T_o , we recover the result of Suezaki and Mori for $T < T_o$. We expect that very close to T_o short-range fluctuations will be dominant. As we move away from the critical region where the FL theory applies, the mean-field approximation should become a reasonable approximation. This crossover has been observed in some systems.⁶ However, in both regimes a decrease of the resistivity upon ordering is predicted, caused by an increase in the relaxation time. This decrease of the resistivity, and the linear relation between $d\rho/dT$ and the specific heat, has been verified in some order-disorder systems such as CuZn (Ref. 3) and CoFe.⁷ The success of this theory suggests that CuZn and CoFe exhibit no significant n_{eff} variation near T_o . On the other hand,

there exist order-disorder systems such as Fe₃Al (Ref. 8) or CoPt,⁹ where there is a slight increase in the resistivity upon ordering. This has been observed in measurements in equilibrium at high temperatures. This situation, also found in antiferromagnets, is characterized by a maximum in the resistivity below T_o or by a negative anomaly in $d\rho/dT$ at the ordering temperature. This effect is probably caused by a decrease of the number of carriers due to the formation of new Brillouin zones upon ordering. In turn, these can give rise to energy gaps at the Fermi level. When two points of the same sheet of the Fermi surface are connected by a superlattice wave vector \mathbf{Q} , an energy gap opens at the Fermi level, the density of states goes down and, accordingly, n_{eff} decreases. Using Eq. (1), this explains the increase of the resistivity caused by ordering in antiferromagnets and certain order-disorder systems. Miwa¹⁰ finds theoretically that n_{eff} is a linear function of the sublattice magnetization below T_o . However, Hall-effect measurements indicate rather that n_{eff} varies like the square of the sublattice magnetization. The latter result has also been obtained theoretically by Ausloos,¹¹

$$n_{\text{eff}} = n_{\text{dis}}(1 - C_0 |\epsilon|^{2\beta}), \quad T < T_o \quad (8)$$

where n_{dis} is the number of carriers per unit volume in the fully disordered state and C_0 is a dimensionless parameter characterizing the energy gap. Using Eq. (1) this leads to a contribution to the critical resistivity going as $|\epsilon|^{2\beta}$, similar to that coming from $1/\tau$ in SM theory. However, the sign of the $|\epsilon|^{2\beta}$ term is opposite in the two cases. It is positive for the energy-gap contribution, and negative for the relaxation-time contribution. Measurements of the ordinary Hall effect can decide whether the gap effect is predominant or not.

Putting together the critical contributions from the relaxation time and from the energy-gap effect on n_{eff} , we obtain a general expression for the resistivity anomaly near an order-disorder phase transition

$$(\rho/\rho_{\text{dis}}) = A_0 + A_1 |\epsilon|^{2\beta} + B_1 |\epsilon|^{-\alpha+1} \quad (9)$$

or

$$(1/\rho_{\text{dis}})d\rho/dT = A_2 |\epsilon|^{2\beta-1} + B_2 |\epsilon|^{-\alpha}. \quad (10)$$

The constants A_1 , B_1 , A_2 , and B_2 take different values and sign above and below T_o . Similar expressions have been proposed to fit the critical resistivity in antiferromagnetic systems.¹² Gap effects may not be visible when measuring $\rho(T)$ at the ordering transition, essentially for two possible reasons.

(a) The topology of the Fermi surface may be such that the ordering wave vector \mathbf{Q} does not span portions of that surface. This has been proposed to explain the "gapless" behavior in CuZn.³

(b) When the measuring temperatures are hundreds of Kelvin, thermal excitation of electrons can easily override gaps of the order of 10–100 meV.

In relation with (b), experiments can be devised to test the dependence of the gap effect on temperature. Sam-

ples can be annealed at a temperature T_Q near T_o long enough for atomic order to reach equilibrium. They are then quenched in water, freezing the atomic order present at T_Q , and $\rho(T_Q, T)$ is then measured at temperatures T equal to 4.2, 77, and 295 K. We can then write

$$n_{\text{eff}} = n_0 + n_1 \exp(-\Delta/k_B T) \quad (11)$$

to model the thermal excitation of electrons across the gap. Here Δ is the gap width. Using Eq. (1) and assuming that the critical behavior is dominated by changes in n_{eff} , rather than in $1/\tau$, we obtain

$$\rho(T_Q, T) \sim [A + B \exp(-\Delta/k_B T)]^{-1} + \rho_{\text{ph}}(T), \quad (12)$$

where $\rho_{\text{ph}}(T)$ is the contribution of phonons, such that $\rho_{\text{ph}}(0) = 0$. Then

$$\frac{\rho(T_Q, 0)}{\rho(T_Q, T) - \rho_{\text{ph}}(T)} = [1 + C \exp(-\Delta/k_B T)]. \quad (13)$$

Equation (13) allows the direct calculation of $\Delta(T_Q)$ from experimental results for $\rho(T_Q, T)$.

II. EXPERIMENTAL METHOD

Our Co-Fe alloys were made from Specpure/Puratronic Johnson and Matthey cobalt and iron. The melting operation was done in a high-vacuum-resistance furnace with a base pressure below 10^{-6} Torr. Mass losses during melting were on the average below 2%, but reached 4% in certain cases. This forced us to perform a final chemical analysis of the ingots to check possible deviations from the nominal value. The final compositions were found to differ by less than 1% from the nominal compositions. This allows us to quote the nominal compositions.

A CsCl ordered structure is known to exist in the range $30 < x < 70$ at. % Co as shown by neutron-diffraction studies.^{13,14} Some controversy arises from the possible existence of ordered CoFe₃ and Co₃Fe phases, reported from resistivity and specific-heat measurements.¹⁵ At the present date these phases have not been observed directly by neutron diffraction and therefore their existence is hypothetical. Our own anisotropic magnetoresistance data seem to support the existence of new ordered phases, close to CoFe₂ and Co₂Fe structures.¹⁶ All samples were homogenized for 24 h in dry hydrogen at 1400 °C. This temperature is about 100 °C below the melting point. After homogenization was completed, the temperature was lowered to 900 °C. Then the hydrogen atmosphere was replaced by a high vacuum [$P \sim (6-7) \times 10^{-6}$ Torr].

The samples were held for 2 h at this temperature to remove any dissolved hydrogen. To obtain maximum atomic order the samples were furnace cooled from 900 °C to room temperature in 8 h.

In these alloys, ordering mainly occurs from a vacancy-jump mechanism. The relaxation time obeys an Arrhenius law¹⁷

$$\tau_{E_{\text{SD}}}(T) = \tau_0 \exp(E_{\text{SD}}/k_B T), \quad (14)$$

where the constant τ_0 and the self-diffusion energy E_{SD} are related to a vacancy formation, and to migration entropies and energies. For Co-Fe alloys, Fishman¹⁸ and Henry¹⁹ obtained $\tau_0 \sim 10^{-14}$ s and $2.7 < E_{SD} < 2.9$ eV. Table I gives the relaxation times calculated from Eq. (14) at several temperatures and also the calculated value of the minimum anneal time 10τ needed to reach equilibrium.¹⁷ It is clear from Table I that perfect order with $S=1$ cannot be obtained with our furnace cooling, because the sample does not stay long enough at temperatures of about 500°C or less for a state of equilibrium to be reached at these temperatures. However, some authors have directly measured the degree of order S of furnace-cooled Co-Fe samples,^{20,21} and reported values greater than 0.9. To lower the degree of order, we quench the samples into a salt solution after allowing enough time for equilibrium to be reached at the quenching temperature T_Q , thus freezing the atomic disorder present at this temperature. Notice that cooling must be fast enough such that appreciable atomic diffusion does not occur during the quenching process. Roughly, quenching times should not exceed $\tau(2.7 \text{ eV}, T_Q)/10$. For $T_Q=900^\circ\text{C}$ this would mean quenching times of the order of milliseconds according to Table I. However, quenching in cold, salted water produces at most quenching rates of about 7000°C/s for thin enough samples and optimum operational conditions. We expect therefore that quenching becomes ineffective for quenching temperatures exceeding 850–900°C. Samples to be quenched are introduced in a quartz tube connected to the diffusion pump by a valve and a flexible bellow at a pressure of 6×10^{-6} Torr. The annealing temperature is kept constant within 1–2°C. After equilibrium at a temperature T_Q has been reached, the valve is closed and the quartz tube quickly immersed into a pan filled with a cold, saturated, salt-water solution where it is smashed. The water is sucked into the tube and cools the sample in a fraction of a second. In most of our samples the resistivity was measured after furnace cooling (ordered state) and after quenching from $T_Q=800^\circ\text{C}$ (disordered state) at $T=4.2, 77,$ and 295 K. In two $\text{Co}_x\text{Fe}_{100-x}$ samples with $x=38$ and 48 at. % Co, we measured $\rho(T_Q, T)$ at $T=4.2, 77,$ and 295 K for several quenching temperatures T_Q above and below the ordering temperature T_0 . Resistivity measurements with a relative resolution of $1:10^4$ were done using a conventional dc four-probe technique. We

TABLE I. Relaxation time τ for two possible self-diffusion energies E_{SD} . We also show the minimum annealing time required to reach equilibrium, defined as 10τ ($E_{SD}=2.9$ eV).

T (°C)	τ , assuming $E_{SD}=2.7$ eV	τ , assuming $E_{SD}=2.9$ eV	Minimum anneal time
500	1 h	20 h	200 h
530	17 min	5 h	50 h
550	6 min	1.5 h	15 h
650	5.5 s	68 s	11 min
880	7 ms	50 ms	0.5 s

also measured $\rho(T)$ in equilibrium at high temperatures through the order-disorder phase transition. A very slow rate of cooling or heating (0.1–0.2°C/min) is needed in order to ensure equilibrium conditions. Under these circumstances, no hysteresis effects were observed in the resistivity runs under heating or cooling cycles.

III. RESULTS AND DISCUSSION

Figure 1 shows the zero-field resistivity of furnace-cooled and quenched alloys at 4.2 K. The quenching temperature is 800°C. Two regions can be distinguished, showing different ordering effects on the resistivity. From $30 < x < 40$ at. % Co, the resistivity of furnace-cooled alloys is larger than that of quenched alloys. From $40 < x < 70$ at. % Co the opposite is true. In the first case, we are probably observing an energy-gap effect. These effects should be easier to observe when the fractional increase of the relaxation time caused by ordering is small. In turn, this means that we must be off stoichiometry. This may explain why this gap effect is observed at $x=35$ at. % Co rather than at 50 at. % Co. Another possibility is that the gap is associated with an Fe_2Co superlattice rather than the FeCo superlattice of CsCl type. Beitel and Pugh²² measured the ordinary Hall coefficient R_0 at 77 and 300 K for a series of furnace-cooled $\text{Co}_x\text{Fe}_{100-x}$ alloys. They found that R_0 diminishes by 16% from 77 to 300 K in a $\text{Co}_{35}\text{Fe}_{65}$ alloy, while $|R_0(77 \text{ K})| \sim |R_0(300 \text{ K})|$ for a $\text{Co}_{50}\text{Fe}_{50}$ alloy. Foner *et al.*²³ have shown that R_0 is almost independent of atomic order in a $\text{Co}_{50}\text{Fe}_{50}$ alloy. As $|R_0|$ is proportional to $1/n_{\text{eff}}$ these results for R_0 and correspondingly for n_{eff} can be understood if an energy gap occurs at the Fermi level for $x=35$ at. % Co, but not for $x=50$ at. % Co. This is consistent with our own results for ρ at 4.2 K described earlier. In Figs. 2 and 3 we study in more detail the behavior of the resistivity in two samples where the gap effect is negligible or preponderant, respectively.

For the $\text{Co}_{48}\text{Fe}_{52}$ sample (Fig. 2) we find $T_0 = 733^\circ\text{C}$

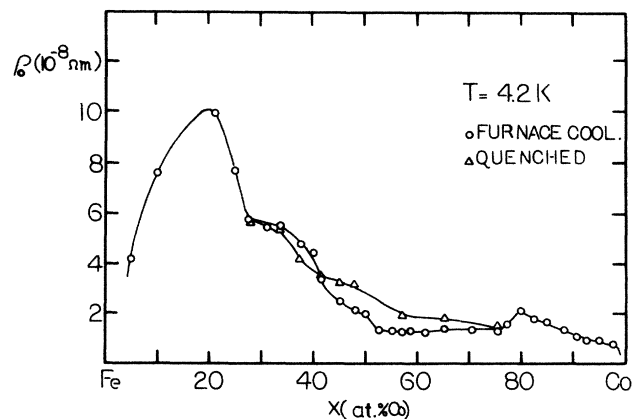


FIG. 1. Zero-field resistivity at 4.2 K for ordered and disordered $\text{Co}_x\text{Fe}_{100-x}$ alloys.

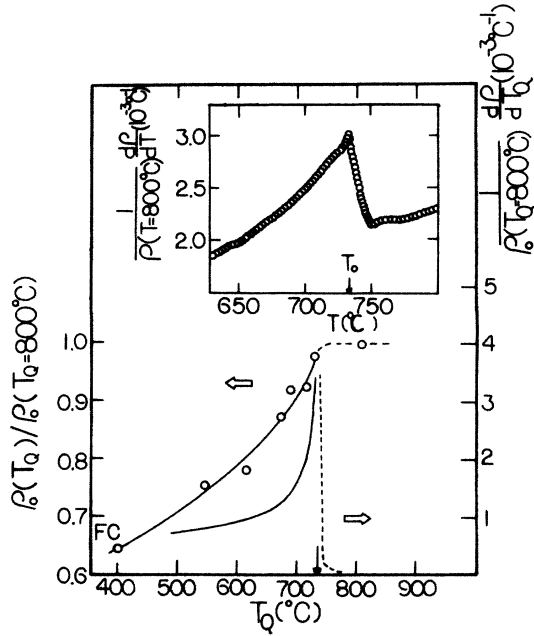


FIG. 2. Normalized zero-field resistivity and its temperature derivative at 4.2 K, for a $\text{Co}_{48}\text{Fe}_{52}$ sample quenched from temperatures T_Q around the ordering temperature T_o . In the inset we show the normalized temperature derivative of the resistivity measured at high temperatures and in equilibrium.

and $\rho(T_Q = 800^\circ\text{C}, 4.2\text{ K}) = 3.24\ \mu\Omega\text{ cm}$. In this sample $\rho_{\text{ord}}(4.2\text{ K}) < \rho_{\text{dis}}(4.2\text{ K})$. As atomic order sets in for $T_Q < T_o$ the resistivity decreases. The solid line through the $\rho(T_Q, 4.2\text{ K})/\rho(T_Q = 800^\circ\text{C})$ data corresponds to a fit of Eqs. (1) and (5) for $T_o = 733^\circ\text{C}$. We use $\beta = 0.312$ as predicted by the three-dimensional Ising model. Notice that in Eq. (5) the reduced temperature is now defined as $\varepsilon = (T_Q - T_o)/T_o$. The $|\varepsilon|^{2\beta}$ term has a negative sign as expected from the increase of the relaxation time as atomic order sets in. We do not have enough data close to T_o to show any rounding or cusp in the resistivity. When we measure $\rho(T_Q, T)$ at 77 and 295 K the resistivity anomaly is of the same type as at 4.2 K; these data are not shown. In the same figure we also show the normalized temperature derivative of the resistivity of quenched samples, $[1/\rho(T_Q = 800^\circ\text{C}, 4.2\text{ K})][d\rho(T_Q, 4.2\text{ K})/dT_Q]$. This quantity has a positive anomaly at $T_Q = T_o$ as obtained in most ferromagnets. In the inset we show the resistivity derivative in equilibrium at a high temperature T . It shows a positive peak at T_o similar to that observed in the quenched samples. These derivative values represent a 20-point fit of the resistivity data to a second-order polynomial. These data agree very well with those of Seehra and Silinsky⁷ for a similar sample. No energy-gap effect is then found at this composition. As observed in Sec. I, the energy-gap effect may be obscured by thermal excitation of the charge carriers across the gap when the resistivity is measured in equilibrium at high temperatures. However this explanation fails for quenched samples where the measurements are done at 4.2 K. Therefore we conclude that the topology of the

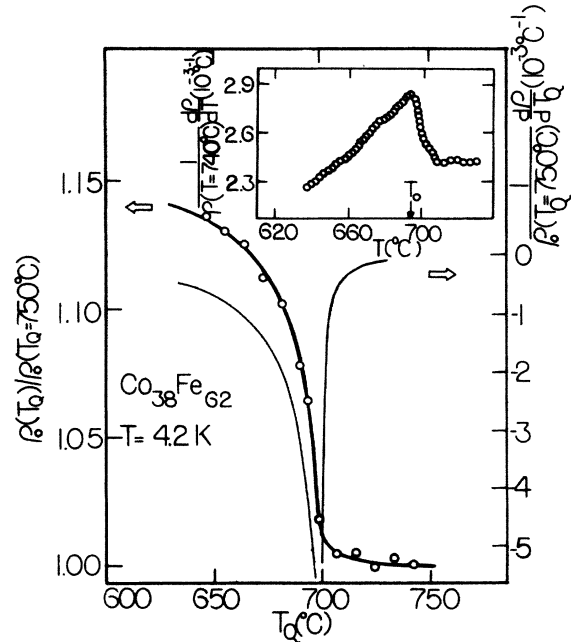


FIG. 3. Normalized zero-field resistivity and its temperature derivative, at 4.2 K, for a $\text{Co}_{38}\text{Fe}_{62}$ sample quenched from temperatures T_Q above and below the ordering temperature T_o . In the inset, we show the normalized temperature derivative of the resistivity, measured at high temperatures in equilibrium.

Fermi surface is such that the superlattice wave-vector \mathbf{Q} does not connect points of that surface at this composition.

Consider now the data for $\text{Co}_{38}\text{Fe}_{62}$ in Fig. 3. Here the resistivity has a pronounced negative derivative with respect to T_Q below T_o , as expected from the energy-gap effect on n_{eff} . In this sample $\rho_{\text{ord}}(4.2\text{ K}) > \rho_{\text{dis}}(4.2\text{ K})$. As atomic order increases for $T_Q < T_o$ the resistivity increases, again as expected when the energy-gap effect is dominant. The solid line through the $\rho(T_Q, T = 4.2\text{ K})$ data is a fit of Eq. (9). We used $\alpha = 0.013$ and $\beta = 0.312$ (3D Ising model).²⁴ The coefficients obtained from the fit are $A_1 = 1.19$ and $B_1 = -1.58$ at $T_Q < T_o$, and $A_1 = -0.271$ and $B_1 = 0.505$ at $T_Q > T_o$. The ordering temperature giving the best fit is $T_o = (700 \pm 0.5)^\circ\text{C}$. Below T_o the coefficient A_1 of the $|\varepsilon|^{2\beta}$ term is strongly positive, leading to the observed increase in the resistivity. The effect of ordering on the relaxation time, below T_o , corresponds to the negative $|\varepsilon|^{-\alpha+1}$ term.

In the inset of Fig. 3 we show our data for $[1/\rho(T = 740^\circ\text{C})](d\rho/dT)$ in equilibrium at a high temperature T . We see that this derivative has a positive peak at T_o , contrary to the negative peak found in the quenched sample, at 4.2 K. This means that, at high temperatures, the gap effect ceases to be dominant, being replaced by the effect of ordering on the relaxation time. At temperatures around 1000 K, gaps of the order of $k_B T \sim 100\text{ meV}$ should barely affect the resistivity. The maximum of $[1/\rho(T = 740^\circ\text{C})](d\rho/dT)$ occurs at $T = 697\text{ K}$. There is a 3 K discrepancy with respect to the critical

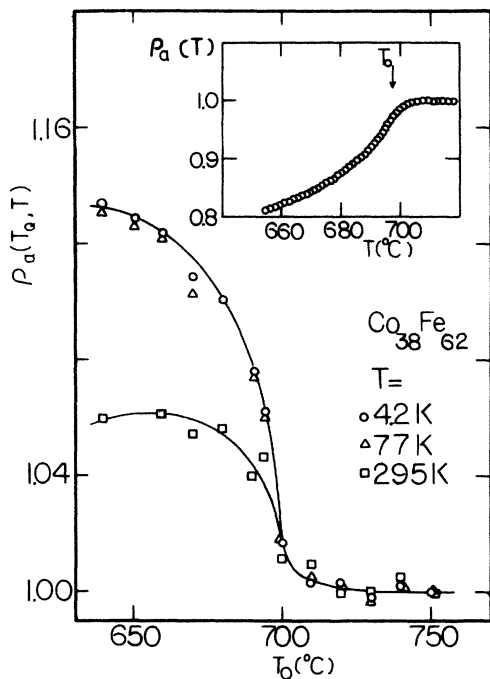


FIG. 4. Normalized zero-field atomic disorder resistivity, $\rho_a(T_Q, T) = [\rho(T_Q, T) - \rho_{ph}(T)] / \rho_{dis}(4.2 \text{ K})$, at 4.2, 77, and 295 K, for a $\text{Co}_{38}\text{Fe}_{62}$ sample quenched from several temperatures T_Q above and below T_o . In the inset we show the equivalent quantity at high temperatures, in equilibrium, as was described in the text.

temperature found when fitting the $\rho(T_Q, 4.2 \text{ K})$ data. It is possible that a small decrease in temperature occurs after we remove the sample from the furnace, before quenching it into water.

Figure 4 shows the quantity $\rho_a(T_Q, T) = [\rho(T_Q, T) - \rho_{ph}(T)] / \rho_{dis}(4.2 \text{ K})$ measured at 4.2, 77, and 295 K for a $\text{Co}_{38}\text{Fe}_{62}$ sample quenched from several temperatures T_Q around the ordering temperature. This normalization removes the phonon contribution to the resistivity at each measuring temperature T . Here $\rho_{ph}(T)$ is defined by

$$\rho_{ph}(T) = \rho(750^\circ\text{C}, T) - \rho(750^\circ\text{C}, 4.2 \text{ K}). \quad (15)$$

The introduction and use of the phonon resistivity $\rho_{ph}(T)$ implicitly assumes that it does not depend on the state of atomic order of the sample. The solid lines through the data are fits of Eq. (9). The displayed quantity should not depend on the measuring temperature T , if the gap effect were independent of T . However, Fig. 4 shows that its value at $T_Q < T_o$ diminishes as we increase the measuring temperature T . Again this suggests the disappearance of the gap effect at high T . At even higher measuring temperatures (see inset, where we show the quantity $\rho_a(T) = [\rho(T) - \rho_{ph}(T)] / \rho_{dis}(4.2 \text{ K})$), the gap effect is approximately absent and the atomic-disorder resistivity increases with increasing T . For the data shown in the inset, $\rho_{ph}(T)$ was assumed to be a linear function of T with such a slope that the alloy-disorder resistivity be independent of T at $T > T_o$. Using values of $\rho(T_Q, T) - \rho_{ph}(T)$ from Fig. 4, we now use Eq. (13) to estimate the width of the energy gap $\Delta(T_Q)$, at a given state of order characterized by T_Q . Data obtained at 4.2 K are used to approximate the corresponding $T=0$ values. The gap width reaches a maximum value of $45 \pm 5 \text{ meV}$ below T_o and remains nearly constant for $T_Q < 680^\circ\text{C}$. In this analysis based on Eq. (13), we neglect the effect of order on τ . Therefore our results for the gap width are only valid close to T_o where the gap effect is dominant.

Finally a comment should be made about the small change in the lattice parameter upon ordering. It is known that the lattice parameter has a maximum increase of 0.2% upon ordering for a $\text{Co}_{50}\text{Fe}_{50}$ alloy.²⁵ In turn, this leads to a decrease of n_{eff} by about 0.6%. The corresponding increase in ρ according to Eq. (1) is very small, when compared with gap or relaxation-time effects (15–20%). We then neglected corrections due to lattice parameter variations in our calculations.

ACKNOWLEDGMENTS

The authors wish to express their thanks to Professor J. B. Sousa for helpful comments concerning the critical behavior of transport properties near order-disorder phase transitions. This work was supported by the Magnetism Technology Center at Carnegie-Mellon University.

*Present address: Instituto de Engenharia de Sistemas e Computadores, R. Alves Redol 9.3^o, 1000 Lisbon, Portugal.

¹D. J. W. Geldart, *Phys. Rev. B* **15**, 3455 (1977).

²J. M. Cowley, *Diffraction Physics* (North-Holland Amsterdam, 1975).

³D. S. Simons and M. B. Salamon, *Phys. Rev. Lett.* **26**, 750 (1971).

⁴M. E. Fisher and J. S. Langer, *Phys. Rev. Lett.* **20**, 665 (1968).

⁵Y. Suezaki and H. Mori, *Prog. Theor. Phys.* **41**, 1177 (1969).

⁶J. B. Sousa, R. P. Pinto, M. M. Amado, J. M. Moreira, M. E. Braga, P. Morin, and M. Ausloos, *J. Phys. F* **10**, 1809 (1980).

⁷M. S. Seehra and P. Silinsky, *Phys. Rev. B* **13**, 5183 (1976).

⁸G. A. Thomas, A. B. Giray, and R. D. Parks, *Phys. Rev. Lett.*

31, 241 (1973).

⁹T. Muto and Y. Takagi, in *Solid State Physics*, edited by F. Seitz and D. Turnbull (Academic, New York, 1955), p. 257.

¹⁰H. Miwa, *Prog. Theor. Phys.* **28**, 108 (1962).

¹¹M. Ausloos, *J. Phys. F* **6**, 1723 (1976).

¹²M. Ausloos, in *Magnetic Phase Transitions*, edited by M. Ausloos and R. J. Elliot (Springer-Verlag, Berlin, 1983), p. 99.

¹³J. A. Oyedelle and M. F. Collins, *Phys. Rev. B* **16**, 3208 (1977).

¹⁴B. G. Lyaschenko, D. F. Litvin, and Y. B. Abov, *Kristallografiya* **6**, 553 (1961) [*Sov. Phys.—Crystallogr.* **6**, 443 (1962)].

¹⁵A. E. Vol, *Constitution and Properties of Binary Metallic Systems* (Gosudarst. Izdatel., Moscow, 1962).

- ¹⁶P. P. Freitas and L. Berger, *J. Magn. Magn. Mater.* **54-57**, 1515 (1986).
- ¹⁷V. Pierron-Bohnes, M. C. Cadeville, and G. Parette, *J. Phys. F* **15**, 1441 (1985).
- ¹⁸S. G. Fishman and D. S. Lieberman, *Phys. Rev. B* **2**, 1451 (1970).
- ¹⁹G. Henry, G. Barreau, and G. Cizeron, *C. R. Acad. Sci.* **16**, 280 (1975).
- ²⁰J. P. Eymery and P. Moine, *J. Phys. (Paris) Lett.* **39**, L23 (1978).
- ²¹B. deMayo, D. W. Forester, and S. Spooner, *J. Appl. Phys.* **41**, 1319 (1970).
- ²²F. P. Beitel and E. M. Pugh, *Phys. Rev.* **109**, 1129 (1958).
- ²³S. Foner, F. E. Allison, and E. M. Pugh, *Phys. Rev.* **109**, 1129 (1958).
- ²⁴S.-k. Ma, *Modern Theory of Critical Phenomena* (Benjamin/Cummings, Massachusetts, 1976).
- ²⁵R. M. Bozorth, *Ferromagnetism* (Van Nostrand, New York, 1951).